ELSEVIER

Journal of Organometallic Chemistry 637–639 (2001) 691–697

Journal of Organometallic Chemistry

www.elsevier.com/locate/jorganchem

Synthesis, X-ray, spectroscopic and a preliminary Suzuki coupling screening studies of a complete series of dppfMX_2 (M = Pt, Pd; X = Cl, Br, I)

Thomas J. Colacot [a,*], Hu Qian [a], Raymundo Cea-Olivares [b], Simon Hernandez-Ortega [b]

[a] *Precious Metals Division, Organometallic Chemicals and Catalysts Development, Johnson Matthey, 2001 Nolte Drive, West Deptford, NJ 08066, USA*

[b] *Instituto de Química, Universidad Nacional Autónoma México Circuito Exterior, Ciudad Universitaria, Mexico D.F. 04510, Mexico*

Received 9 April 2001; received in revised form 1 May 2001; accepted 2 May 2001

Abstract

A complete series of dppfMX_2 (M = Pt, Pd; X = Cl, Br, I) compounds have been synthesized using different routes, and characterized fully. The synthesis of dppfPdI_2 has been achieved by reacting Pd(COD)Cl_2 with dppf in the presence of NaI. X-ray structures of dppf$PdBr_2$ and dppfPdI_2 have also been reported for the first time in this study. A preliminary Suzuki coupling screening study reveals that dppfPdX_2 compounds are superior to the conventional Ph_3P-based catalysts and bidentate phosphine-based ligands. Reactions carried out under in situ conditions also gave a similar trend, but their respective activities were much lower than that of the fully formed catalysts. © 2001 Elsevier Science B.V. All rights reserved.

Keywords: 1,1′-Bis(diphenylphosphino)ferrocene; Suzuki coupling; NMR; X-ray; Pt and Pd complexes of dppf

1. Introduction

The applications of 1,1′-bis(diphenylphosphino)ferrocene, dppf, and related ligands in C–C and C–heteroatom coupling reactions have been reviewed very recently [1]. A couple of years ago, our laboratory had reported the syntheses and X-ray characterization of dppfPtI_2 and dppf$PtPh_2$ [2]. Interestingly, for both these complexes, the P–Pt–P bite angles (Fig. 1) were larger than that of the reported structure of dppf$PtCl_2$ [3]. This was quite unexpected, as the steric bulk of the X_2 groups in (P–P)PtX_2 (P–P = bidentate phosphine) should theoretically decrease the P–Pt–P bite angles. In Pd chemistry, about 15 years ago, Hayashi reported that dppf$PdCl_2$ behaved in a far superior manner than the conventional mono- and bidentate phosphines in their C–C coupling reactions involving a Grignard or zinc reagent [4]. The remarkable success of this catalyst was attributed to its larger P–Pd–P bite angle (99.07°), and is referred to as 'magic catalyst' by Gan and Hor in the book, *Ferrocenes* [5]. However, a recent study from Hayashi's laboratory suggested that smaller X–Pd–X bond angles might be more important than the larger bite angles [6].

Since Pt is not a good system to study the C–C coupling reactions, we decided to synthesize a complete series of dppfMX_2 (M = Pt, Pd; X = Cl, Br, I) and systematically compare the catalytic activities of these complexes as a function of their bite angles and X–Pd–X bond angles. This study also reports the X-ray crystal structures of dppfPdX_2 (X = Br, I), in order to obtain complete data on these series.

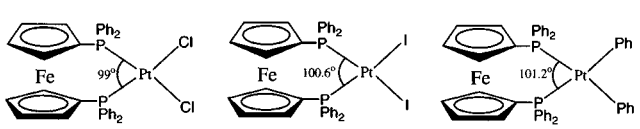

Fig. 1. Bite angles of dppfPtX_2 (X = Cl, I, Ph) complexes, a comparison.

* Corresponding author. Tel.: +1-609-384-7185; fax: +1-609-384-7035.

E-mail address: colactj@jmusa.com (T.J. Colacot).

PII: S0022-328X(01)00981-0

Table 1
Crystal data [a] and structure refinement parameters for $dppfPdX_2$

	$dppfPdI_2$	$dppfPdBr_2$
Empirical formula	$C_{34}H_{28}Br_2FeP_2Pd\cdot CH_3OH$	$C_{34}H_{28}Br_2FeP_2Pd\cdot 0.5\ CH_2Cl_2$
Formula weight	945.60	863.04
Temperature (K)	293	293
Crystal system	triclinic	monoclinic
Space group	$P\bar{1}$	$C2/c$
Unit cell dimensions		
a (Å)	10.012(3)	33.822(5)
b (Å)	10.761(4)	10.504(3)
c (Å)	17.672(5)	18.871(2)
α (°)	86.17(2)	90
β (°)	76.19(2)	104.17(1)
γ (°)	66.55(2)	90
V (Å^3)	1695(1)	6500(2)
Z	2	8
D_{calc} (g cm^{-3})	1.852	1.764
Absorption coefficient (mm^{-1})	2.900	3.663
$F(000)$	914	3400
Crystal size (mm)	$0.40\times0.20\times0.04$	$0.26\times0.20\times0.18$
Crystal color/habit	dark-red/lamina	red/block
Index ranges	$0\le h\le11$, $-11\le k\le12$, $-20\le l\le21$	$0\le h\le40$, $0\le k\le12$, $-22\le l\le21$
Max/min transmission	0.375, 0.888	0.403, 0.456
Data collected	6332	5832
No. of parameters refined	374	376
$R(F\ge2\sigma(I))$	0.0512	0.0632 [b]
wR^2	0.0714	0.0976 [c]
S	1.28	0.998 [d]
Largest difference peak and hole (e Å^{-3})	1.64 (0.73 Å close to methanol) and −1.42	0.618 and −0.535

[a] Graphite monochromated Mo–Kα radiation, $\lambda = 0.71073$ Å.
[b] $R = \Sigma||F_o|-|F_c||/\Sigma|F_o|$, $wR = \{\Sigma[w(F_o-F_c)^2]/\Sigma w(F_o)^2\}^{1/2}$.
[c] $wR^2 = \{\Sigma[w(F_o^2-F_c^2)^2]/\Sigma w(F_o^2)^2\}^{1/2}$.
[d] $S = \{\Sigma[w(F_o^2-F_c^2)^2]/(n-p)\}^{1/2}$; where n = no. of reflections and p = no. of parameters refined.

2. Experimental

2.1. General procedures

The syntheses of $dppfMX_2$ were carried out in an inert atmosphere using conventional Schlenk techniques in conjunction with the Vacuum Atmospheres Company glove box (Model HE 493/MO-5). The precursors such as dppf, $LPtX_2$ (L = NBD, COD; X = Cl, Br, I) and $LPdX_2$ (L = NBD, COD; X = Cl, Br) were obtained from our production facility. All solvents and chemicals were purchased from Alfa Aesar or Aldrich. The elemental assays were done at E & R Microanalytical Laboratory, NY and Robertson Microlit, NJ. Melting points were determined using the Thomas–Hoover melting point apparatus using sealed capillaries and are uncorrected.

^{1}H-, ^{13}C- and ^{31}P-NMR spectral data were collected on a Varian XL-300 FT-NMR spectrometer operating at 300.1, 75.5 and 121.1 MHz, respectively. The ^{1}H- and ^{13}C-shifts were referenced to Me_4Si in the solvent, while ^{31}P-shifts were referenced to an external standard, 85% H_3PO_4. The Suzuki coupling products were analyzed using a Perkin–Elmer Autosystem XL Gas Chromatograph equipped with a FID detector. An SPB-5 column (30 m length, 0.25 mm diameter) with a temperature program (140 °C/0.50 min; 35 °C min^{-1} to 200 °C, hold for 1 min; 40 °C min^{-1} to 300 °C, hold for 4 min) was used to have a run time of 10 min.

Table 2
Selected bond lengths (Å) and bond angles (°) for $dppfPdX_2$

$dppfPdBr_2$		$dppfPdI_2$	
Bond lengths			
Pd–P(1)	2.297(2)	Pd–P(1)	2.326(2)
Pd–P(2)	2.303(3)	Pd–P(2)	2.327(2)
Pd–Br(2)	2.4628(12)	Pd–I(1)	2.650(1)
Pd–Br(1)	2.4849(13)	Pd–I(2)	2.643(1)
Fe–C(6)	2.000(8)	Fe–C(25)	2.006(7)
Fe–C(10)	2.010(9)	Fe–C(27)	2.063(9)
Fe–C(1)	2.015(8)	Fe–C(29)	2.036(8)
Fe–C(7)	2.028(9)	Fe–C(31)	2.034(10)
Fe–C(5)	2.028(8)	Fe–C(33)	2.067(9)
Fe–C(2)	2.029(8)	Fe–C(26)	2.038(9)
Fe–C(9)	2.054(10)	Fe–C(28)	2.062(9)
Fe–C(4)	2.061(8)	Fe–C(30)	2.007(7)
Fe–C(3)	2.065(9)	Fe–C(32)	2.061(8)
Fe–C(8)	2.092(10)	Fe–C(34)	2.033(9)
P(1)–C(1)	1.811(8)	P(1)–C(1)	1.821(8)
P(1)–C(11)	1.814(8)	P(1)–C(25)	1.820(7)
P(1)–C(17)	1.829(8)	P(2)–C(19)	1.827(8)
P(2)–C(6)	1.803(8)	P(1)–C(7)	1.830(11)
P(2)–C(29)	1.828(8)	P(2)–C(13)	1.816(10)
P(2)-C(23)	1.841(9)	P(2)–C(30)	1.810(7)
Bond angles			
P(1)–Pd–P(2)	98.77(8)	P(1)–Pd–P(2)	99.9(1)
P(1)–Pd–Br(2)	170.09(7)	P(1)–Pd–I(1)	83.9(1)
P(2)–Pd–Br(2)	90.85(7)	P(2)–Pd–I(1)	176.1(1)
P(1)–Pd–Br(1)	83.12(7)	I(1)–Pd–I(2)	87.7(1)
P(2)–Pd–Br(1)	177.82(7)	P(1)–Pd–I(2)	169.4(1)
Br(2)–Pd–Br(1)	87.22(4)	P(2)–Pd–I(2)	88.6(1)
C(1)–P(1)–C(11)	100.4(4)	C(7)–P(1)–Pd	113.3(3)
C(1)–P(1)–C(17)	100.7(4)	C(25)–P(1)–Pd	121.7(3)
C(11)–P(1)–C(17)	108.4(4)	C(7)–P(1)–C(25)	100.3(4)
C(1)–P(1)–Pd	124.2(3)	C(19)–P(2)–Pd	120.3(3)
C(11)–P(1)–Pd	109.9(3)	C(30)–P(2)–Pd	114.2(3)
C(17)–P(1)–Pd	111.9(3)	C(19)–P(2)–C(30)	101.4(3)
C(6)–P(2)–C(29)	105.3(4)	C(1)–P(1)–Pd	112.0(3)
C(6)–P(2)–C(23)	102.2(4)	C(1)–P(1)–C(7)	108.3(4)
C(29)–P(2)–C(23)	103.4(4)	C(1)–P(1)–C(25)	99.6(3)
C(6)–P(2)–Pd	114.7(3)	C(13)–P(2)–Pd	110.2(3)
C(29)–P(2)–Pd	112.6(3)	C(13)–P(2)–C(19)	102.7(5)
C(23)–P(2)–Pd	117.2(3)	C(13)–P(2)–C(30)	106.6(4)

Table 3
Synthetic routes for dppfMX_2 complexes with yield

Compounds [a]	Method	Solvent	Yield (%)	Color	M.p. (°C dec.)
dppf$PdCl_2 \cdot n CH_2Cl_2$	(NBD)$PdCl_2$ + L	CH_2Cl_2	95	Brick-red	290
dppf$PdCl_2$	(NBD)$PdCl_2$ + L	Acetone	96	Brick-red	260
dppf$PdBr_2$	(NBD)$PdCl_2$ + L	Acetone	95	Purple–red	295
dppf$PdBr_2 \cdot n CH_2Cl_2$	(COD)$PdCl_2$ + L	CH_2Cl_2	98	Purple–red	305
dppfPdI_2	dppf$PdCl_2$ + NaI	Acetone	98	Violet–red	310
dppf$PtCl_2 \cdot n CH_2Cl_2$	(COD)$PtCl_2$ + L	CH_2Cl_2	95	Yellow	335
dppf$PtBr_2 \cdot n CH_2Cl_2$	(COD)$PtBr_2$ + L	CH_2Cl_2	97	Yellow	310
dppf$PtI_2 \cdot n CH_2Cl_2$	(COD)PtI_2 + L	CH_2Cl_2	96	Yellow	320

[a] Excellent elemental assays were obtained for all the compounds ($n = 0.25$–1 mol).

2.2. Synthesis of $Cp_2Fe(PPh_2)_2PtX_2 \cdot nCH_2Cl_2$ ($X = Cl$, Br, I; $n = 0.25$–1)

To a stirred solution of 1,1′-bis(diphenylphosphino)ferrocene, dppf (2.8 g, 5.05 mmol) in anhydrous CH_2Cl_2 (50 ml), (NBD or COD)PtX_2 (5.0 mmol) was added all at once and stirred for 2 h. The reaction mixture was then concentrated to one-fifth of its original volume under reduced pressure. Et_2O (50 ml) was added to the same mixture to obtain a yellow crystalline solid, which was filtered, washed with Et_2O (10 ml × 3) and dried under vacuum to obtain dppfPtX_2 (yield ca. 95%).

2.3. Syntheses of $Cp_2Fe(PPh_2)_2PdX_2 \cdot nCH_2Cl_2$ ($X = Cl$, Br)

To a suspension of (COD or NBD)PdX_2 (X = Cl, Br, 5.0 mmol) in 50 ml CH_2Cl_2, dppf (2.8 g, 5.05 mmol) was added all at once. The mixture was stirred at room temperature for 2 h, and then the volume was reduced to 10 ml by vacuum. Et_2O (50 ml) was added to the above mixture and stirred for another 10 min. The solid thus formed was filtered, washed with Et_2O (10 ml × 3) and dried under vacuum to obtain analytically pure samples of dppf$PdX_2 \cdot n CH_2Cl_2$ (X = Cl, Br) in ca. 95% yield.

2.4. Syntheses of $Cp_2Fe(PPh_2)_2PdX_2$ ($X = Cl$, Br)

The reaction was carried out under identical conditions as described above, except the fact that anhydrous acetone was used as the solvent. The products, dppfPdX_2 (Cl, Br) were isolated in over 95% yield as crystalline solids.

2.5. Synthesis of $Cp_2Fe(PPh_2)_2PdI_2$

To a stirred suspension of dppf (5.6 g, 10.1 mmol) in anhydrous acetone (100 ml), (COD)$PdCl_2$ (10.0 mmol) was added and stirred for 1 h, to obtain a red solid. To this mixture, NaI (3.29 g, 22.0 mmol) was added and stirred for another 30 min to obtain a violet-colored reaction mixture. The reaction mixture was then concentrated to 20 ml under reduced pressure, followed by the addition of Et_2O (100 ml). The resulting precipitate was filtered, washed with water (20 ml), 40% aqueous EtOH (100 ml), EtOH (50 ml) and Et_2O (50 ml) to obtain a violet crystalline sample of dppfPdI_2 (96%).

2.6. General experimental for Suzuki screening

In a typical reaction, 0.5 mmol of bromoacetophenone, 0.6 mmol of phenyl boronic acid and 1.5 mmol of K_2CO_3 taken in Radley's Carousel tubes containing a magnetic stir bar were degassed for 5 min under nitrogen atmosphere. To this, was added 1 mol% equivalent of the catalyst in 5 ml toluene. The mixture was allowed to stir at 70 °C for about 2 h under nitrogen. About 1 ml of this mixture was filtered using a silica gel plug, followed by washing the plug with 1 ml of MeCN. The products were analyzed with the help of a GC equipped with an auto-sampler.

2.7. X-ray structural analyses

X-Ray structural analyses of dppf$PdBr_2$ and dppfPdI_2: single crystals of dppf$PdBr_2$ and dppfPdI_2 were obtained by the diffusion method using CH_2Cl_2–hexane and CH_2Cl_2–MeOH solvent combinations, respectively. The crystals were mounted on a Siemens P4/PC diffractometer using highly oriented graphite monochromatic Mo–Kα ($\lambda = 0.71073$ Å) radiation. The unit cell parameters summarized in Table 1, were obtained by least-squares fit of up to 40 accurately centered reflections in the range $4° \leq 2\theta \leq 25°$, and the intensity data were collected at 293 K in the range $3° \leq 2\theta \leq 50°$, using the ω:2θ scan technique.

Three standard reflections measured after every 97 reflections show no significant variation in the intensities. The data set was corrected for Lp and absorption effects (face-indexed numerical method for dppfPdBr$_2$ and ψ-scans for dppfPdBr$_2$). The structures were solved by direct methods and refined by full-matrix least-squares using an isotropic thermal parameters for all non-hydrogen atoms [7]. All the hydrogen atoms were included as fixed contributions and not refined. Their idealized positions were generated from the geometry about the attached carbon atoms, and forced to ride on it with a fixed isotropic temperature factor, $U = 1.2$ times the U_{eq} of the parent C-atom and C–H distance of 0.96 Å. The structure of dppfPdI$_2$ was refined by SHELXL-90 [8], while the structure of dppfPdBr$_2$ was refined by using SHELXL-97 [9]. The final models converged as shown in Table 1, while atomic coordinates ($\times 10^4$) and equivalent isotropic displacement coefficients (Å$^2 \times 10^3$) for dppfPdBr$_2$ and dppfPdCl$_2$ are deposited as Supplementary material. Table 2 gives the selected bond angles and bond lengths of dppfPdX$_2$ (X = Br, I).

3. Results and discussion

Using 1,5-cyclooctadiene and norbornadiene complexes of MX$_2$ (M = Pt, X = Cl, Br, I; M = Pd, X = Cl, Br), dppfMX$_2$ have been synthesized in very good purity with excellent yield (Table 3). When the reactions were carried out in CH_2Cl_2, the products contain 0.25–1 mol equivalent of the solvent in the crystal lattice. However, the reactions carried out in acetone produced solvent-free products as evidenced by NMR and elemental assay. This is fairly significant as chlorinated solvents can interfere with the catalytic activities of the catalyst in certain cases. All these compounds were characterized unambiguously by FT-IR, multinuclear NMR and elemental assay.

Although dppfPtI$_2$ could easily be prepared from starting materials such as (COD)PtI$_2$ or (NBD)PtI$_2$, it was practically impossible to synthesize dppfPdI$_2$ using the analogous route as the corresponding NBD- or (COD)PdI$_2$ could not be synthesized (Scheme 1). However, dppfPdI$_2$ was synthesized in nearly quantitative yield with very good purity by using an in situ exchange of the chloride in dppfPdCl$_2$ with slight excess of NaI (Scheme 2). The yield of dppfPdI$_2$ was far superior to that reported recently for the analogous bidentate complex, dpppPdI$_2$ [10]. The byproduct, NaCl and excess NaI were then washed away with water. It is interesting to note that we could not synthesize NBD- and (COD)PdI$_2$ from the corresponding halides by halogen exchange reaction. The color of the dppfPdCl$_2$ is brick-red, while that of the iodide is violet–red. The bromide has a color in between that of the chloride and iodide.

The NMR spectral data of all these complexes are listed in Table 4. The phosphorus chemical shift values of both Pt and Pd complexes show a clear trend where the phosphorus atoms in the chlorides are less shielded, while those of the bromides and iodides are relatively more shielded. This could be very well explained based on the electronegativities of the respective halogens [11]. Interestingly, the ^{31}P-chemical shifts of the Pd complexes have a higher frequency than those of the Pt complexes, which could be explained on their relative positions in the periodic table [11]. The $^2J_{P-P'}$ couplings (hidden P–P couplings) also follow a similar trend, although dppfPdBr$_2$ is an exception. However, these values were derived by computer simulation experiments, similar to what we reported earlier [2].

The ORTEP diagram for dppfPdBr$_2$ and dppfPdI$_2$ are shown in Figs. 2 and 3, respectively. As in the reported case of dppfPdCl$_2$, both the bromide and iodide have slightly distorted square planar geometry [4]. Unlike the Pt series, the dppfPdX$_2$ (X = Cl, Br, I) compounds have more or less identical Pd–P–Pd bite angles (98.8–99.9°) and X–Pd–X angles (87.2–87.8°).

The results of the Suzuki coupling screening studies are listed in the bar chart (Fig. 4). Both dppfPdCl$_2$ and dppfPdBr$_2$ have shown the highest activity under identical conditions. This is expected, based on their identical bite angles and X–Pd–X angles. However,

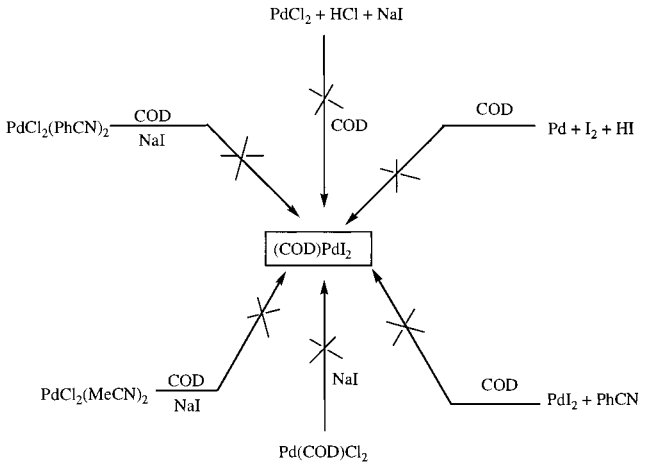

Scheme 1. Attempted synthesis of NBD- and (COD)PdI$_2$.

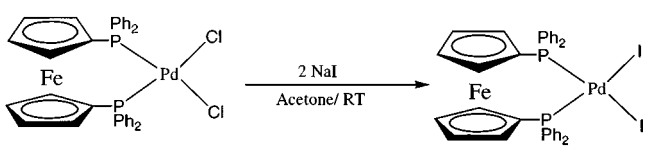

Scheme 2. High yield synthesis of dppfPdI$_2$.

Table 4
NMR spectral data of $dppfMX_2$, a comparison

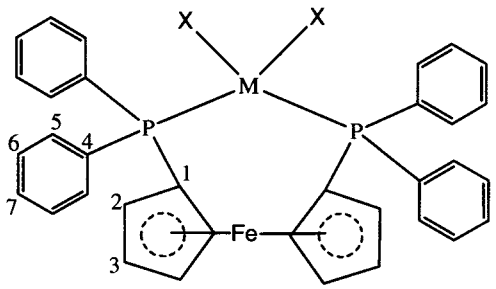

Atom	$dppfPtCl_2$	$dppfPtBr_2$	$dppfPtI_2$	$dppfPdCl_2$	$dppfPdBr_2$	$dppfPdI_2$
P (δ) ppm	13.3	12.5	10.1	34.5	31.5	25
$^2J_{P-P'}$ (Hz)	11.2	7.3	7	19.7	22.6	5.3
$^1J_{Pt-P'}$ (Hz)	3778.7	3729.3	3551.8			
Cl (δ) ppm	73.1	73.7	74.4	74.4	75.1	75.8
$^1J_{P-Cl}$ (Hz)	70.7	66.7	62.2	56.5	54.3	48.5
$^3J_{P'-Cl}$ (Hz)	0.2	3.8	3.4	7.1	6.6	6.5
H2 (δ) ppm	4.21	4.2	4.16	4.22	4.2	4.16
C2 (δ) ppm	76.2	76.1	75.6	76.7	76.7	76.6
$^2J_{P'-C2}+{}^4J_{P'-C2}$ (Hz)	10.7	10.4	17.1	10.7	10.7	10.5
H3 (δ) ppm	4.39	4.37	4.31	4.42	4.4	4.37
C3 (δ) ppm	74.4	74.3	73.5	74.5	74.4	74.1
$^3J_{P'-C3}+{}^5J_{P'-C3}$ (Hz)	8	8		7.8	7.5	7.4
C4 (δ) ppm	131.3	132.2	133.1	132.3	133.2	134.5
$^1J_{P-C4}$ (Hz)	67.1	66.6	64.8	57.7	56.8	54.5
$^3J_{P'-C4}$ (Hz)	~0	1	1	~0	~0	0.5
$^2J_{Pt'-C4}$ (Hz)	26.9	30.6	34.6			
H5 (δ) ppm	7.86	7.89	7.9	7.89	7.9	7.89
C5 (δ) ppm	135.3	135.3	135.2	135.3	135.4	135.5
$^2J_{P'-C5}+{}^4J_{P'-C5}$ (Hz)	11.1	10.9	10.7	11.8	11.5	11.3
H6 (δ) ppm	7.42	7.43	7.38	7.44	7.44	7.43
C6 (δ) ppm	128.3	128.2	127.7	128.5	128.4	128.2
$^3J_{P'-C6}+{}^5J_{P'-C6}$ (Hz)	11.6	11.6	11.7	11.6	11.4	11.3
H7 (δ) ppm	7.52	7.52	7.45	7.54	7.53	7.51
C7 (δ) ppm	131.6	131.6	130.1	131.7	131.6	131.4
$^4J_{P'-C7}$ (Hz)	2.6	2.8	<3	2.7	<3 (broad)	2.8

the activity of the corresponding iodide was lower than that of the chloride and bromide. This is quite unexpected and we are not able to provide a valid explanation for this finding. Presumably, the relatively lower solubility of the iodide in toluene and the more unstable nature of the catalyst in solution might be responsible for the relatively low activity. The activities of the other bidentate phosphine complexes such as $dppbPdCl_2$ and $dppePdCl_2$ were lower than that of the dppf complexes under identical conditions, although these ligands were fairly effective for the reaction of phenyl boronic acid with bromoacetophenone. The Ph_3P-based Pd complex, $(Ph_3P)_2PdCl_2$, also gave the coupled product, but the rate of conversion was low in comparison to that of the $dppfPdCl_2$ complex. None of the $dppfPtX_2$ complexes have given any coupled products. The reactivity differences of the catalysts are more evident at lower temperatures. Biphenyl was also detected as a byproduct (2–10%) in most cases.

We also examined the activities of these ligands (Ph_3P, dppe, dppb and dppf) under in situ conditions using $Pd(OAc)_2$ and Pd_2dba_3 as precursors. Although dppf was the best ligand under identical conditions, the activities of all the ligands were much lower than that of their fully formed catalysts. Moreover, the fully formed catalysts gave cleaner products. For example, the Ph_3P–$Pd(OAc)_2$ system has produced

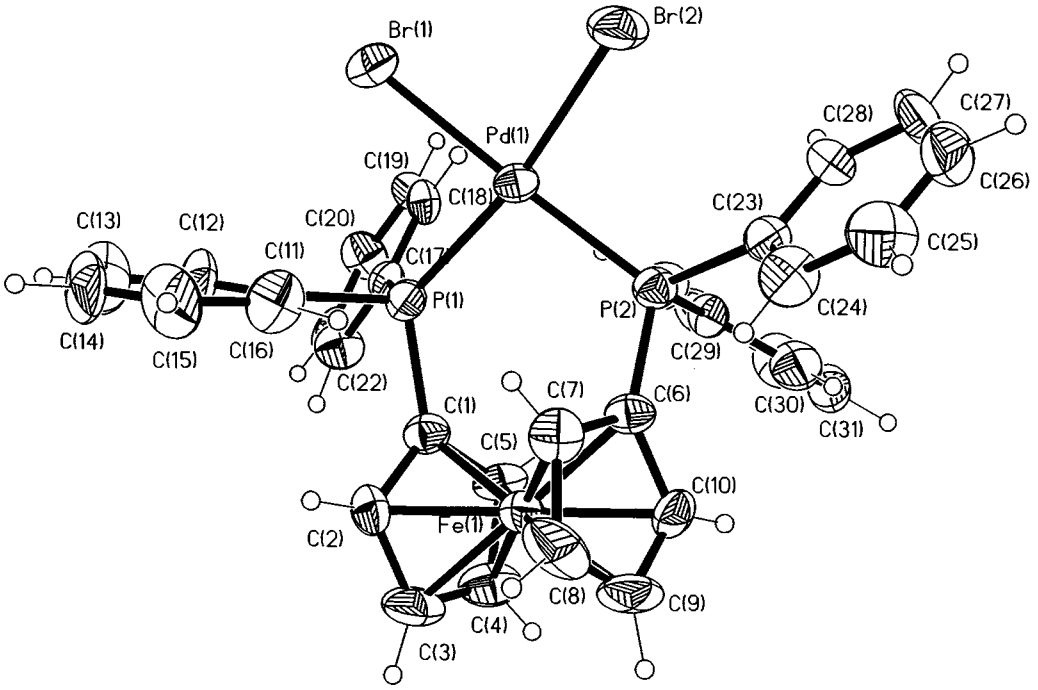

Fig. 2. ORTEP diagram of $Cp_2FePdBr_2$, showing 30% probability ellipsoids.

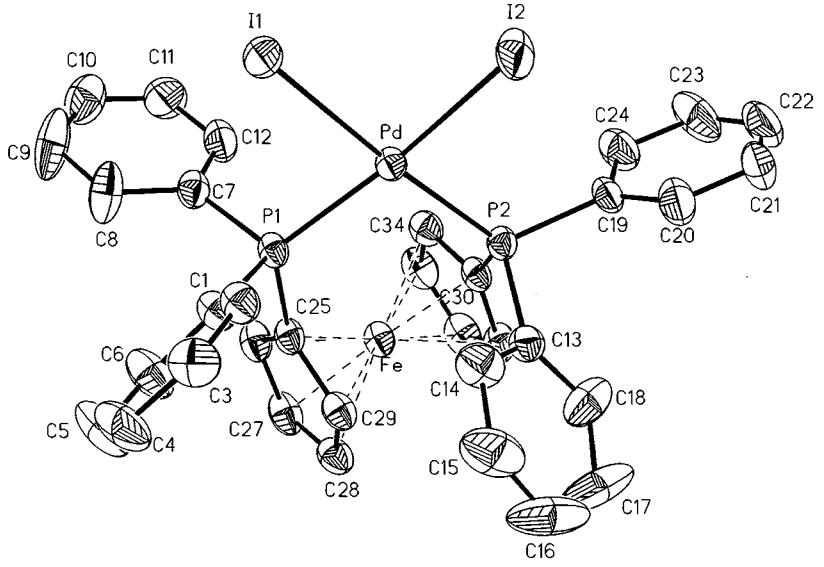

Fig. 3. ORTEP diagram of Cp_2FePdI_2, showing 30% probability ellipsoids.

some small amount of Ullman-coupled product. We also observed that the rate of stirring and rate of heating affect the rate of conversion and the product distribution.

4. Supplementary material

Crystallographic data for the structural analysis have been deposited with the Cambridge Crystallographic Data Centre, CCDC nos. 119112 and 119113, respectively, for compounds $dppfPdBr_2$ and $dppfPdI_2$. Copies of this information may be obtained free of charge from The Director, CCDC, 12 Union Road, Cambridge CB2 1EZ, UK (Fax: +44-1223-336033; e-mail: deposit@ccdc.cam.ac.uk or www: http://www.ccdc.cam.ac.uk).

Acknowledgements

Dr W.H. Tamblyn and Dr R.A. Teichman of Johnson Matthey are acknowledged for their support and encouragement in this work.

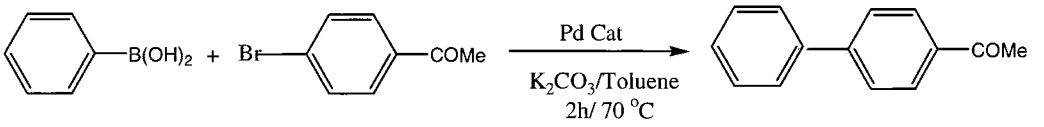

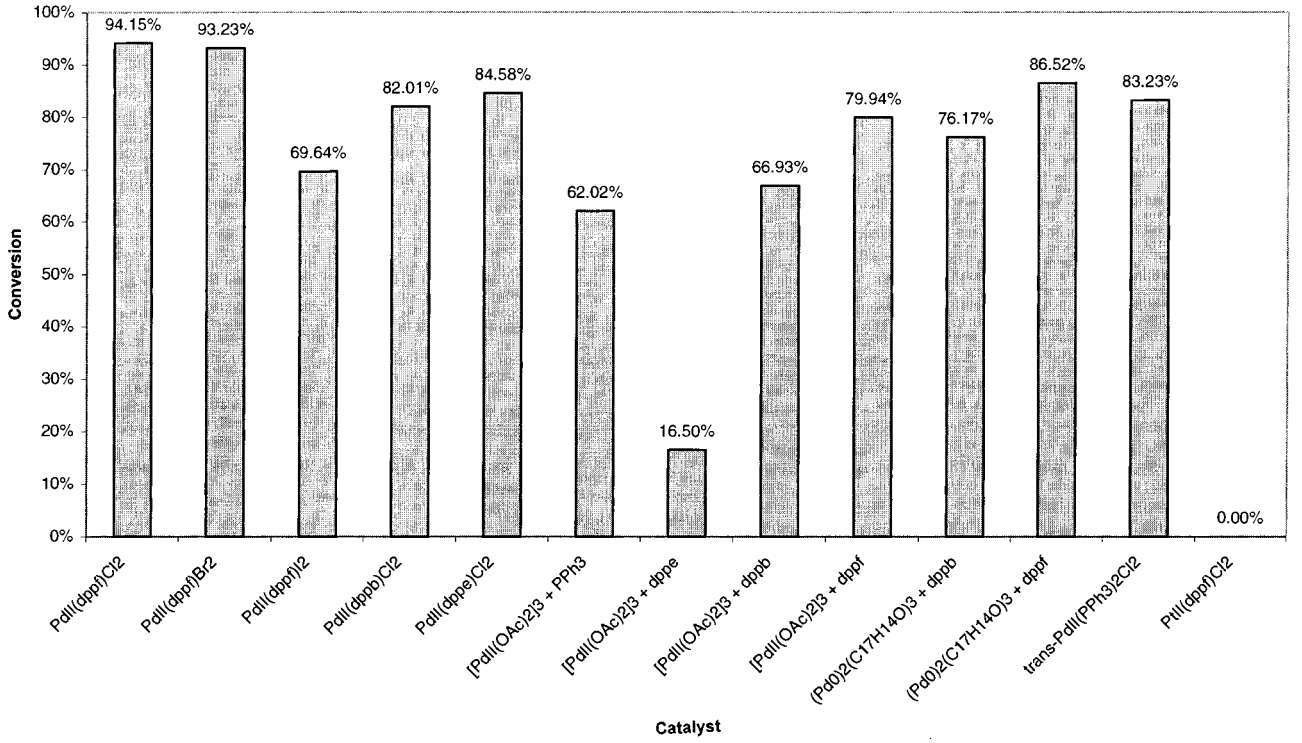

Fig. 4. Bar chart representing the relative conversions of the Suzuki coupling reaction, in the presence of various Pd catalysts.

References

[1] T.J. Colacot, Platinum Met. Rev. 45 (2001) 22 (see references therein).
[2] T.J. Colacot, R.A Teichman, R. Cea-Olivares, J.-G. Alvarado-Rodríguez, R.A. Toscano, W.J. Boyko, J. Organomet. Chem. 557 (1998) 169 (see references therein).
[3] G.M. De Lima, C.A.L. Filguerias, Transition Met. Chem. 20 (1995) 380.
[4] T. Hayashi, M. Konishi, Y. Kobori, M. Kumada, T. Higuchi, K. Hirotsu, J. Am. Chem. Soc. 106 (1984) 158.
[5] K.-S. Gan, T.S. Hor, in: A. Togni, T. Hayashi (Eds.), Ferrocenes, VCH, New York, 1995, pp. 1–104.
[6] M. Ogasawara, K. Yoshida, T. Hayashi, Organometallics 19 (2000) 1567.
[7] A. Altomare, G. Cascarano, C. Giacovazzo, A. Guagliardi, M.C. Burla, G. Polidori, M. Camalli, J. Appl. Crystallogr. 27 (1994) 435.
[8] G.M. Sheldrick, SHELXTL/PC User's Manual, Siemen's Analytical X-rays Instruments, Inc., Madison, WI, USA, 1990.
[9] G.M. Sheldrick, SHELXL-97, Program for the Refinement of Crystal Structures, University of Göttingen, Göttingen, Germany, 1997.
[10] J. Barkely, M. Ellis, S.J. Higgins, M.K. McCart, Organometallics 17 (1998) 1725.
[11] P.S. Pregosin, R.W. Kunz, in: P. Diehl, E. Fluck, R. Kosfed (Eds.), NMR, Basic Principles and Progress, Springer-Verlag, Berlin, 1979, p. 16.